

Structural damping of composite materials using combined FE and lamb wave method

B.S. Ben¹, B.A. Ben², S.H. Kweon³ and S.H. Yang^{*3}

¹Department of Mechanical Engineering, National Institute of Technology, Warangal, 506004, India

²Department of Mechanical Engineering (AUCE), Andhra University, Visakhapatnam, 530003, India

³School of Mechanical Engineering, Kyungpook National University, Daegu 702-701, South Korea

(Received August 20, 2012, Revised June 2, 2014, Accepted July 20, 2014)

Abstract. The article presents the methodology for finding material damping capacity at higher frequency and at relatively lower amplitudes. The Lamb wave dispersion theory and loss less finite element model is used to find the damping capacity of composite materials. The research has been focused on high frequency applications materials. The method was implemented on carbon fiber reinforced polymer (CFRP) and glass fiber reinforced polymer (GFRP) plates. The Lamb waves were generated using ultrasonic pulse generator setup. The hybrid method has been explored in this article and the results have been compared with bandwidth methods available in the literature.

Keywords: lamb wave; acoustic emission; vibration; carbon fibers; glass fibers; damping

1. Introduction

The damping capacity of a material is the fundamental property for designing and manufacturing structural components in dynamic applications. Materials with high damping capacity are very desirable to suppress mechanical vibration and transmission of waves, thus decreasing noise and maintaining the stability of structural systems. Experimental and analytical characterization of damping is not easy, even with conventional structural materials, and the anisotropic nature of composite materials makes it even more difficult. Experimental approaches range from laboratory bench-top methods to portable field inspection techniques, whereas analytical techniques vary from simple mechanics-of-materials methods to sophisticated three-dimensional finite-element approaches. This article presents a combined Lamb wave and finite element method for finding damping capacity of a material using ultrasonic pulse generator experimental setup.

Damping in composites involves a variety of energy dissipation mechanisms that depend on vibrational parameters such as frequency and amplitude and these are studied with nondestructive evaluation. In fiber-reinforced polymers, the most important damping mechanisms have been studied by Chen *et al.* (2003).

The nondestructive evaluation (NDE) techniques such as radiography, acoustic emission,

*Corresponding author, Professor, E-mail: syang@knu.ac.kr

thermal NDE methods, optical methods, vibration damping techniques, corona discharge and chemical spectroscopy, have also been applied to characterize the fiber-reinforced composites by Summerscales (1987). Among these techniques, the vibration damping method, which is based on energy dissipation theory, has been increasingly used for measuring damping capacity. The principle of the method is based on the theory of energy dissipation. According to the theory, quality of interfacial adhesion in composites can be evaluated by measuring the part of energy dissipation contributed by the interfaces, assuming that the interface part can be obtained by separating those of matrix and fiber from the total composites. The energy dissipation of a material can be evaluated by the damping of the material.

Nowick *et al.* (1972) summarized the techniques currently used for measuring vibration damping of materials and structures. The techniques for the measurement of damping often deal with natural frequency or resonant frequency of a system. In general, all apparatus for the investigation of vibration can be categorized as free vibration (or free decay) and forced vibration. Free vibration is executed by a system in the absence of any external input except the initial condition inputs of displacement and velocity, Botelho *et al.* (2006). For example, it is possible to have a wire sample gripped at the top, and have a large weight hanging freely at the bottom; this system can be set either into longitudinal or torsional oscillation. The latter represents the well-known “torsion pendulum”, developed by Ting-Sui K, in which the strain at any point can be expressed in terms of the angular twist of the inertia member. For a forced vibration, a periodic exciting force is applied to the mass. When the resonant frequency is achieved, the loss angle is obtainable directly from the width of the resonance peak at half-maximum in a plot of (amplitude) versus frequency. Gibson (1992) presented typical forced vibration techniques include the free-free beam technique and the piezoelectric ultrasonic composite oscillator technique (PUCOT) (Marx 1951, Harmouche *et al.* 1985, Gremaud *et al.* 2001). These techniques have been applied to dynamic mechanical analysis (DMA) which is a widely used technique in polymer studies, and has attracted even more attention for interface characterization. However, the instrument is relatively expensive and cannot be operated at a high frequency which can reflect more information from the tested materials.

Ultrasounds are one of the classical ways used to examine and characterize materials. As far composite materials are concerned, the acoustic propagation through anisotropic multilayered media has become the subject of intensive study because of their application to nondestructive evaluation, geophysics, etc.

The damping of fiber reinforced composite materials has been studied extensively by (Guan *et al.* 2001, Mu *et al.* 2006). All of the published results for continuous fiber reinforced composites show that when strain levels are low the damping characteristics do not depend on strain amplitude but are dependent on fiber orientation, temperature, moisture absorption, frequency, and matrix properties. Fiber properties have only minimal effects. However, for discontinuous fiber reinforced composites it has been shown that the damping characteristics in the fiber direction are much greater than that obtained continuous fiber reinforced composites. It is commonly accepted that the main sources of damping in a composite material come from microplastic or viscoelastic phenomena associated with the matrix and slippage at the interface between the matrix and the reinforcement.

Composite materials fall into two categories: fiber reinforced and particle (or whisker) reinforced composite materials. Both are widely used in advanced structures. Among the various kinds of composites, glass fiber-reinforced polymer (GFRP) and carbon fiber-reinforced polymer (CFRP) composites have become more and more important in engineering applications because of

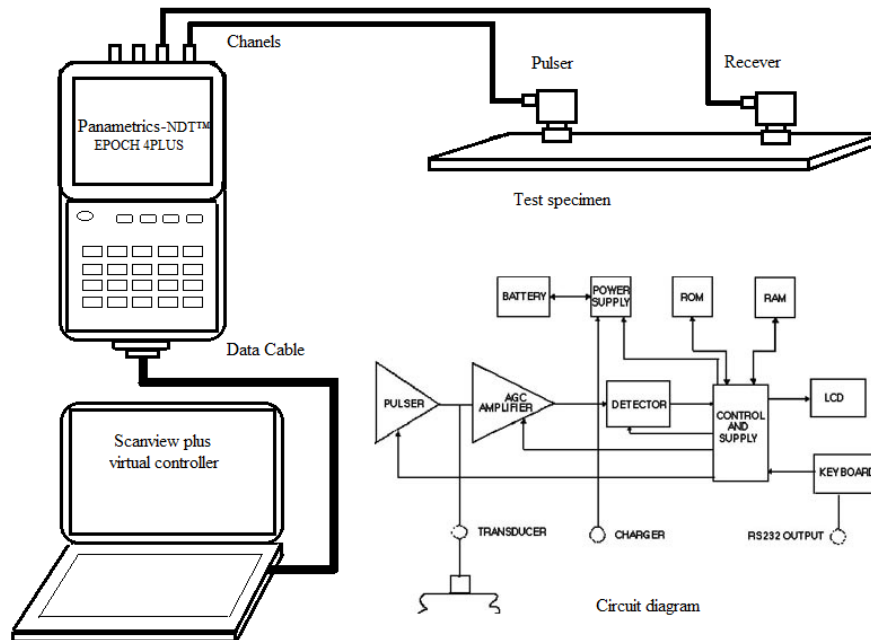


Fig. 1 Schematic representation of experimental setup

their low cost, light weight, high specific strength and good corrosion resistance.

This paper will emphasize viscoelastic damping, which appears to be the dominant mechanism in undamaged polymer composites vibrating at small amplitudes. The bandwidth method using ultrasonic acoustic emission was able to find the damping properties to the maximum range of frequency but it has a problem with overlapping of modes and it is difficult to identify them. To overcome this problem a hybrid method is developed by combining finite element and Lamb wave dispersion theory. The damping capacity of composite material found in the bandwidth method has been validated with the developed hybrid method at various critical modes of frequency.

2. Experimental setup

2.1 Ultrasonic pulse generator

In this work carbon fiber/epoxy (CFRP) and glass fiber/epoxy (GFRP) were tested for their damping properties. The specimens of dimensions $120 \times 30 \times 2$ mm were fabricated by the standard process, Michael 1998. The laminate consists of 12 plies and each ply consisting of woven fiber mat with epoxy layer of thickness 0.2mm. A schematic diagram of the experimental setup is shown in Fig. 1. The test specimen is clamped at one end on a cantilever support. The transducers were placed on the test specimen at a distance of 80 mm from each other. The shear wave transducer was coupled to the specimen using a honey glycerine couplant made by Panametrics. The couplant was able to provide transmission of a normal incident shear wave to the specimen. We used the pitch-catch radio frequency (RF) test method, which uses dual-element sensors (DIC-0408) with a 1 KHz to 4 MHz frequency range. A point-contact sensor (DIC-0408) with an 8 mm

diameter was used in the test setup where one element transmits a burst of acoustic waves into the test piece, and a separate element receives the sound propagated across the test piece between the transducer tips as shown in Fig. 2. Both the actuation and the data acquisition were performed using a portable Panametrics NDT™ EPOCH 4PLUS and a laptop PC running Scanview plus software as a virtual controller.

2.2 Calibration of ultrasonic pulse generator for optimal lamb wave generation

The Panametrics-NDT™ EPOCH 4PLUS is capable of producing ultrasonic sound waves and is equipped with four channels i.e., Device, Pulser, Receiver and Waveform. Each channel is having editable parameters tabulated below.

Channels		Editable Parameters			
Device	Unit	Angle	Thickness		
Pulser	Mode	Energy	Wave Type	Frequency	
Receiver	Gain	Broad band	Low pass	High pass	By pass
Waveform	Range	Rectification	Offset		

The optimal driving frequency for different specimens is obtained by varying different editable parameters shown in the above table. Fig. 3 shows the calibration of ultrasonic pulse generator for test specimens based on its fitted peak value and similarly it is calibrated for various materials. Curves have been plotted between pulser frequency and signal amplitude at receiver for different materials to find optimal driving frequency and it is shown in Fig. 4. A Histogram representation of percentage amplitude of waveform at constant gain which is used to attain a trend line for optimal driving frequency for different materials is shown in Fig. 4 and the % amplitude of the waveform at various pulser frequencies is taken as Bin range (0-820 kHz) at constant gain 55 (db)



Fig. 2 Experimental setup

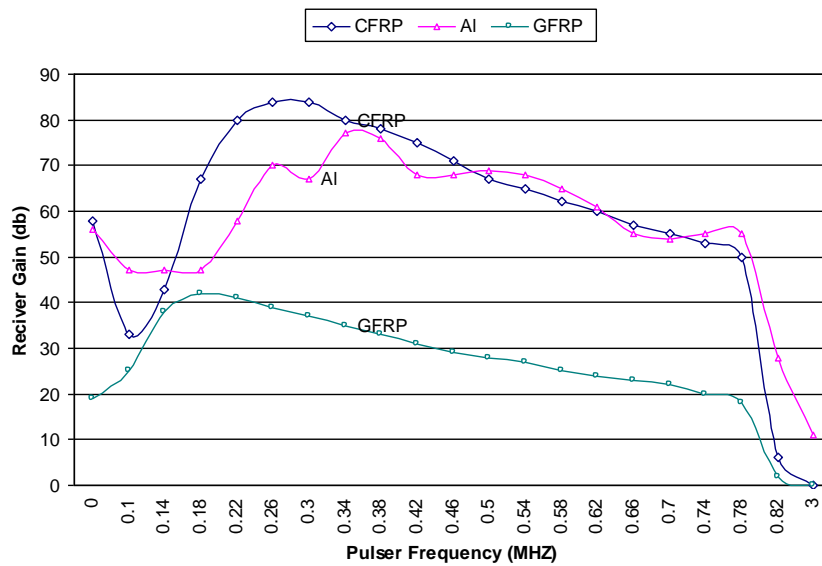


Fig. 3 Optimal driving frequency selection for different materials

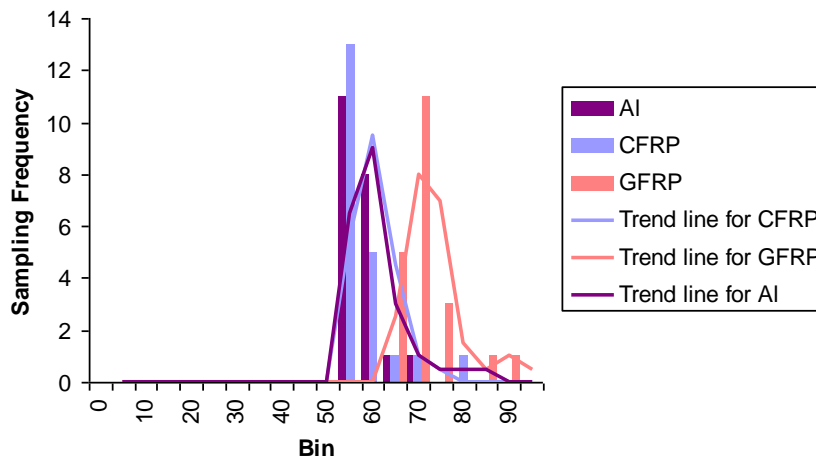


Fig. 4 Histogram representation of % amplitude of waveform at constant gain

for different materials.

The frequency of the transducer to be used is proportional to the acoustic impedance of the layer. Materials such as graphite or fiberglass with low impedance require lower frequency transducers than metal skin layers. It is observed that the frequencies in the range of 100 KHz to 460 kHz have been useful in most of the testing. The higher frequencies are used for thinner and metallic layers.

2.3 Material properties calculated using experimental setup

The basic material property Young’s modulus is obtained from the ultrasonic pulse generator

experimental setup. The instrument finds the Acoustic Emission (AE) velocities travelling in the material which will be very useful for determining the material properties (Birt 1998, Ratnam *et al.* 2009, McIntire 1991, Krautkramer *et al.* 1983). The Young's modulus of the test specimen is determined using the relation given in Eq. (1).

$$E_1 = \frac{V_T^2 \rho (1 + \nu_{12})(1 - 2\nu_{12})}{1 - \nu_{12}} \quad (1)$$

$$E_2 = \frac{V_L^2 \rho (1 + \nu_{12})(1 - 2\nu_{12})}{1 - \nu_{12}}$$

where V_L and V_T are longitudinal and transverse velocity of Lamb waves traveling in the material respectively, ρ is material density and ν_{12} is Poisson's ratio. Table 1 presents the material properties of the test specimens.

3. Bandwidth method

Damping in composites involves a variety of energy dissipation mechanisms that depend on vibrational parameters such as frequency and amplitude and these are studied with nondestructive evaluation. Damping in a system can be determined by noting the maximum response, i.e., the response at the resonance frequency as indicated by the maximum value of R_v . Fig. 5 illustrate the Bandwidth method of damping measurement where, damping in a system is indicated by the sharpness or width of the response curve in the vicinity of a resonance frequency ω_r , designating the width as a frequency increment (i.e., $\Delta\omega = \omega_2 - \omega_1$) measured at the "half-power point" (i.e., at a value $(R/\sqrt{2})$) and the damping ratio ζ can be estimated by using band width in the relation given by

$$\zeta = \frac{\Delta\omega}{2\omega_r} \quad (2)$$

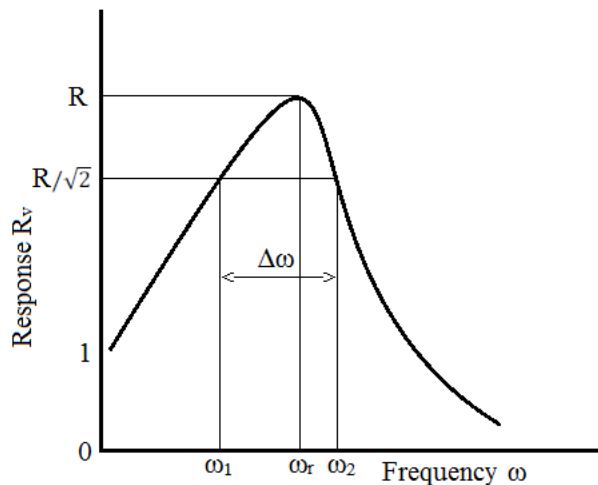


Fig. 5 Response curve showing bandwidth at "half-power point"

For i_{th} mode damping ratio is given by

$$\zeta_i = \frac{1}{2} \frac{\Delta\omega_i}{\omega_i} \tag{3}$$

The differential equation of motion for the System with viscous damping when the excitation is a force $F = F_o \sin \omega t$ applied to the system, is given by

$$m\ddot{x} + c\dot{x} + kx = F_o \sin \omega t \tag{4}$$

Eq. (4) represents the forced vibration of an undamped system and the resulting motion occurs at the forcing frequency ω . When the damping coefficient c is greater than zero, the phase between the force and resulting motion is different than zero which leads to the phase angle δ , presented in Eq. (5) as a function of the frequency ratio ω/ω_r and for several values of the fraction of critical damping ζ , Blake 2010.

$$\delta = \tan^{-1} \frac{2\zeta(\omega/\omega_r)^3}{1 - (\omega^2/\omega_r^2) + (2\zeta\omega/\omega_r)^2} \tag{5}$$

4. Finite element model for free vibration analysis of a laminated composite plate

The oscillatory motion is a characteristic property of the structure and it depends on the distribution of mass and stiffness in the structure. If damping is present, the amplitude of oscillations will decay progressively and if the magnitude of damping exceeds a certain critical value, the oscillatory character of the motion will cease altogether. On the other hand, if damping is absent, the oscillatory motion will continue indefinitely, with the amplitudes of oscillations depending on the initially imposed disturbance or displacement. The oscillatory motion occurs at certain frequencies known as natural frequencies or characteristic values, and it follows well defined deformation pattern known as mode shapes or characteristic modes. The study of such free vibration is very important in finding the dynamic response of elastic structures.

By assuming the external force vector \vec{p} to be zero and the displacement to be harmonic as:

$$\vec{Q} = \underline{\underline{Q}} \cdot e^{i\omega t} \tag{6}$$

and the free vibration equation is given by

$$[[k] - \omega^2[M]]\vec{Q} = \vec{0} \tag{7}$$

where $\underline{\underline{Q}}$ represents the amplitude of the displacement \vec{Q} (mode shape or eigen vector) and ω denotes the natural frequency of vibration. Eq. (7) is called a linear algebraic eigenvalue problem since neither $[k]$ nor $[M]$ is a function of the circular frequency ω , and it will have a nonzero solution for $\underline{\underline{Q}}$ provided that the determinant of coefficient matrix $([k] - \omega^2[M])$ is zero, i.e.

$$|[k] - \omega^2[M]| = 0 \tag{8}$$

where $[k]$ is stiffness matrix and $[M]$ is mass matrix. As said above the oscillatory motion is a characteristic property of the structure and it depends on the distribution of mass and stiffness in

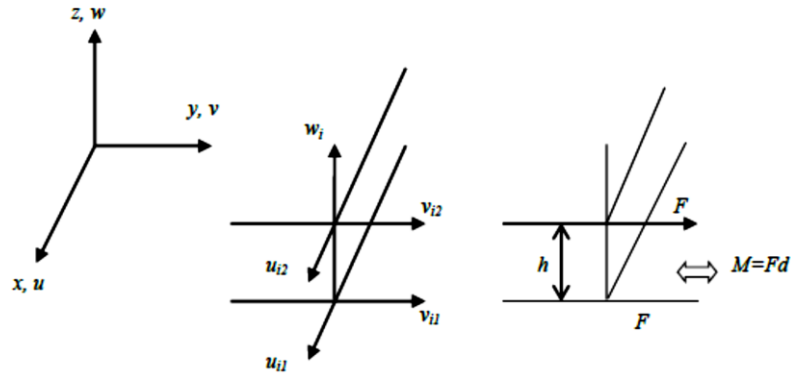


Fig. 6 Plate element with displacement degrees of freedom

the structure, so the stiffness and mass matrix are derived as follows.

The plate bending developed in this section is shown in Fig. 6 where x , y , and z describe the global coordinate of the plate and u , v , and w are the displacements. h is the plate thickness. The xy plane is parallel to the midsurface plane prior to deflection.

The displacement of any point in the plate can be expressed as

$$u = u(x, y, z) \quad (9)$$

$$v = v(x, y, z) \quad (10)$$

$$w = w(x, y, z) \quad (11)$$

That is the in plane displacement u and v vary through the plate thickness as well as with in the xy -plane while the transverse displacement w remains constant through the plate thickness (Owen *et al.* 1987, Kwon 1989). In order to interpolate the displacement using shape functions and nodal displacements, two different interpolations are needed: one interpolation within the xy -plane and the other in the z -axis. For the xy -plane interpolation, shape function $N_i(x,y)$ are used where subscript i varies depending on the number of nodes on the xy -plane. On the other hand, shape function $H_j(z)$ are used for interpolation along the z -axis, where subscript j varies depending on the number of nodes along the plate thickness. Because two inplane displacement are functions of x , y , and z , both shape functions are used while the transverse displacement uses shape functions $N_i(x,y)$. Using isoparametric element with mapping of ξ, η -plane onto xy -plane and ζ -axis to z -axis, the three displacements can be expressed as

$$u = \sum_{i=1}^{N_1} \sum_{j=1}^{N_2} N_i(\xi, \eta) H_j(\zeta) u_{ij} \quad (12)$$

$$v = \sum_{i=1}^{N_1} \sum_{j=1}^{N_2} N_i(\xi, \eta) H_j(\zeta) v_{ij} \quad (13)$$

$$w = \sum_{i=1}^{N_1} N_i(\xi, \eta) w_i \quad (14)$$

In which N_1 and N_2 are the number of nodes in xy -plane (ξ, η -plane) and z -axis (ζ -axis), respectively. In addition, the first subscript for u and v denotes the node numbering in terms of xy -plane (ξ, η -plane) and the second subscript indicates the node numbering in terms of z -axis (ζ -axis). In the present study, $N_1=4$ and $N_2= 2$. That is four-node quadrilateral shape function are employed for the xy -plane (ξ, η -plane) interpolation and linear shape function are employed for the z -axis (ζ -axis) interpolation. Nodal displacement u_{i1} and v_{i1} are displacement on the bottom surface of the plate element and u_{i2} and v_{i2} are displacement on the top surface. As seen in Eqs. (12) through (14), there is no rotational degree of freedom for the present plate bending element.

In the present formulation, both bending strain energy and transverse shear strain energy are included. The bending strains and transverse shear strain are expressed in terms of displacements.

$$\{\epsilon_b\} = \begin{Bmatrix} \epsilon_x \\ \epsilon_y \\ \gamma_{xy} \end{Bmatrix} = \begin{bmatrix} \frac{\partial}{\partial x} & 0 & 0 \\ 0 & \frac{\partial}{\partial y} & 0 \\ \frac{\partial}{\partial y} & \frac{\partial}{\partial x} & 0 \end{bmatrix} \begin{Bmatrix} u \\ v \\ w \end{Bmatrix} \tag{15}$$

$$\{\epsilon_s\} = \begin{Bmatrix} \gamma_{yz} \\ \gamma_{xz} \end{Bmatrix} = \begin{bmatrix} \frac{\partial}{\partial z} & 0 & \frac{\partial}{\partial x} \\ 0 & \frac{\partial}{\partial z} & \frac{\partial}{\partial y} \end{bmatrix} \begin{Bmatrix} u \\ v \\ w \end{Bmatrix} \tag{16}$$

Where $\{\epsilon_b\}$ is the bending strain and $\{\epsilon_s\}$ is the transverse shear strain. The normal strain along the plate thickness ϵ_z is omitted here.

Substitution of displacement, Eqs. (12) through (14), into the kinematic equations, Eqs. (19) and (20), with $N_1= 4$ and $N_2= 2$ expresses both bending and shear strain in the following way.

$$\{\epsilon_s\} = [B_b] \{d^e\} \tag{17}$$

Where

$$[B_b] = [[B_{b1}] \quad [B_{b2}] \quad [B_{b3}] \quad [B_{b4}]] \tag{18}$$

$$[B_b] = \begin{bmatrix} H_1 \frac{\partial N_i}{\partial x} & 0 & H_2 \frac{\partial N_i}{\partial x} & 0 & 0 \\ 0 & H_1 \frac{\partial N_i}{\partial y} & 0 & H_2 \frac{\partial N_i}{\partial y} & 0 \\ H_1 \frac{\partial N_i}{\partial y} & H_1 \frac{\partial N_i}{\partial x} & H_2 \frac{\partial N_i}{\partial y} & H_2 \frac{\partial N_i}{\partial x} & 0 \end{bmatrix} \tag{19}$$

$$\{d^e\} = \{\{d_1^e\} \quad \{d_2^e\} \quad \{d_1^e\} \quad \{d_2^e\}\}^T \tag{20}$$

$$\{d_i^e\} = \{u_{i1} \quad v_{i1} \quad u_{i2} \quad v_{i2} \quad w_i\} \tag{21}$$

$$\{\varepsilon_s\} = [B_s] \{d^e\} \quad (22)$$

Where

$$[B_s] = [[B_{s1}] \quad [B_{s2}] \quad [B_{s3}] \quad [B_{s4}]] \quad (23)$$

$$[B_{si}] = \begin{bmatrix} N_i \frac{\partial H_1}{\partial z} & 0 & N_i \frac{\partial H_2}{\partial z} & 0 & \frac{\partial N_i}{\partial x} \\ 0 & N_i \frac{\partial H_1}{\partial z} & 0 & N_i \frac{\partial H_2}{\partial z} & \frac{\partial H_2}{\partial y} \end{bmatrix} \quad (24)$$

The constitutive equation for the isotropic material is

$$\{\sigma_b\} = [D_b] \{\varepsilon_b\} \quad (25)$$

$$\{\sigma_b\} = \{\sigma_x \quad \sigma_y \quad \tau_{xy}\}^T \quad (26)$$

$$[D_b] = \frac{E}{1-\nu^2} \begin{bmatrix} 1 & \nu & 0 \\ \nu & 1 & 0 \\ 0 & 0 & \frac{1-\nu}{2} \end{bmatrix} \quad (27)$$

For the bending components

$$\{\sigma_s\} = [D_s] \{\varepsilon_s\} \quad (28)$$

Where

$$\{\sigma_s\} = \{\tau_{yz} \quad \tau_{xz}\}^T \quad (29)$$

$$[D_s] = \frac{E}{2(1+\nu)} \begin{bmatrix} 1 & 0 \\ 0 & 1 \end{bmatrix} \quad (30)$$

Where Eq. (27) is the material property matrix for the plane stress condition as usually assumed for the plate bending theory and for a fibrous composite, the material property matrices is given by

$$[D_b] = \begin{bmatrix} D_{11} & D_{12} & 0 \\ D_{12} & D_{22} & 0 \\ 0 & 0 & D_{33} \end{bmatrix} \quad (31)$$

In which

$$D_{11} = \frac{E_1}{1-\nu_{12}\nu_{21}} \quad (32)$$

$$D_{12} = \frac{E_1\nu_{21}}{1-\nu_{12}\nu_{21}} \quad (33)$$

$$D_{22} = \frac{E_2}{1 - \nu_{12}\nu_{21}} \tag{34}$$

$$D_{33} = G_{12} \tag{35}$$

And

$$[D_s] = \begin{bmatrix} G_{13} & 0 \\ 0 & G_{12} \end{bmatrix} \tag{36}$$

Here, 1 and 2 denote the longitudinal and transverse directions of the composite, respectively. Further E is the elastic modulus, G_{ij} the shear modulus of the i - j plane and ν_{ij} is Poisson's ratio for strain in the j -direction when stressed in the i -direction. There are five independent material properties for Eqs. (31) through (36) because of the reciprocal relation

$$\frac{\nu_{12}}{E_1} = \frac{\nu_{21}}{E_2} \tag{37}$$

by minimum potential energy approach the stiffness matrix of the element $[k^{(e)}]$ is expressed as

$$[k^{(e)}] = \int_{\Omega^e} [B_b]^T [D_b] [B_b] \partial\Omega + \int_{\Omega^e} [B_s]^T [D_s] [B_s] \partial\Omega \tag{38}$$

where Ω is the plate domain.

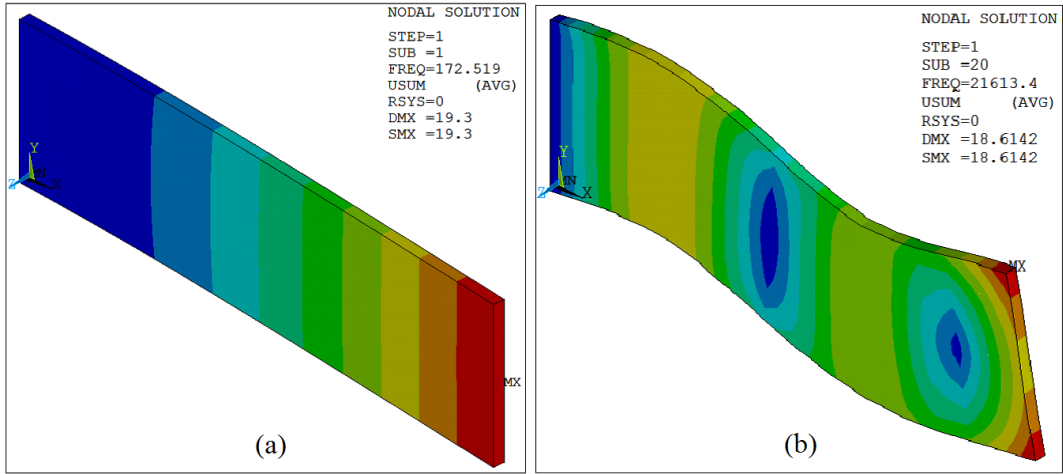
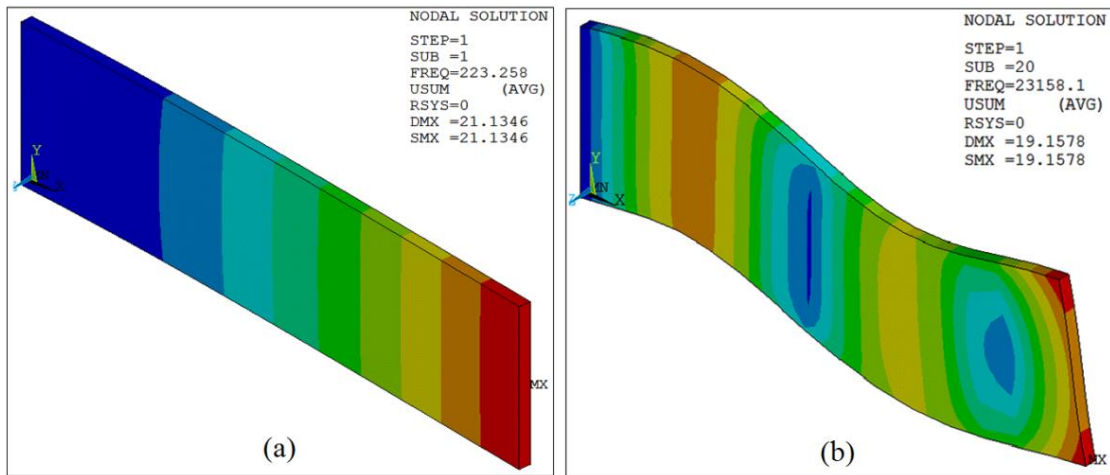
Similarly the mass matrix is given by

$$[M^{(e)}] = \frac{\rho A t}{9} \begin{bmatrix} 4 & 2 & 1 & 2 \\ 2 & 4 & 2 & 1 \\ 1 & 2 & 4 & 2 \\ 2 & 1 & 2 & 4 \end{bmatrix} \tag{39}$$

where A element area, t thickness of element and ρ density of material. Using the above discussed method natural frequencies are computed for composite plates. The computation has been carried out using MathematicaTH software and the inputs for the solution have been taken from the experimental data discussed in the previous sections. A finite element model was also developed in ANSYS to correlate with theoretical model. The modal analysis was carried out using Block Lanczos method for thirty subsets and shell-190 has been used as meshing element. Fig. 7 and Fig. 8 shows the first and twentieth mode of natural frequency of the two materials, GFRP and CFRP respectively.

5. Lamb wave model for laminated composite plate

There are two groups of Lamb waves, symmetric and anti-symmetric, that satisfy the wave equation and boundary conditions for this problem and each can propagate independently of the other. In the following section, analytical models for Lamb wave propagation have been derived, which relate the velocity of the wave-front to the actuating frequency.

Fig. 7 GFRP specimen's 1st and 20th mode of natural frequencyFig. 8 CFRP specimen's 1st and 20th mode of natural frequency

The most descriptive way to represent the propagation of a Lamb wave in a particular material is with their dispersion curves, which plot the phase and group velocities versus the excitation frequency given by Dalton *et al.* 2001. The derivation of these curves begins with the solution to the wave equation for the anti-symmetric Lamb wave formulated as seen in Eq. (40)

$$\frac{\tan(qh)}{\tan(ph)} = \frac{(k^2 + q^2)^2}{4k^2qp} \quad (40)$$

where $p^2 = \frac{\omega^2}{c_t^2} - k^2$, $q^2 = \frac{\omega^2}{c_l^2} - k^2$, and $k = \frac{\omega}{c_{phase}}$

For a laminated composite with the 1-axis defined as the fiber direction, the 2-axis transverse to the fiber, and the 3-axis being out of the plane of the plate, the stress-strain relationship in an individual laminate is given by Daniel *et al.* (1994).

$$\begin{bmatrix} \sigma_1 \\ \sigma_2 \\ \tau_6 \end{bmatrix} = \begin{bmatrix} Q_{11} & Q_{12} & 0 \\ Q_{12} & Q_{22} & 0 \\ 0 & 0 & Q_{66} \end{bmatrix} \begin{bmatrix} \varepsilon_1 \\ \varepsilon_2 \\ \gamma_6 \end{bmatrix} \quad (41)$$

Where σ and τ represent the normal and shear stresses, respectively, and ε and γ represent the normal and shear strain, respectively. The Q_{ij} are the reduced stiffness components and are defined in terms of the engineering parameters as

$$\begin{aligned} Q_{11} &= E_1 / (1 - \nu_{12}\nu_{21}) \\ Q_{22} &= E_2 / (1 - \nu_{12}\nu_{21}) \\ Q_{12} &= \nu_{12}E_1 / (1 - \nu_{12}\nu_{21}) \end{aligned} \quad (42)$$

where E_1 and E_2 are the Young's moduli in the longitudinal and transverse directions, respectively, and ν_{12} and ν_{21} are the major and minor Poisson's ratios, respectively. The Poisson's ratios in Eq. (42) are not independent quantities and are related to each other by

$$\nu_{21} = \frac{E_2}{E_1} \nu_{12} \quad (43)$$

The in-plane stiffnesses for the entire plate, A_{11} and A_{22} , are obtained by integrating the Q_{ij} through the thickness of the plate. These stiffness values are defined as

$$A_{ij} = \int_{-h/2}^{h/2} (Q'_{ij})_k dz, \quad i, j = 1, 2, \quad (44)$$

where h is the plate thickness and the subscript k represents each lamina. The Q'_{ij} are the transformed stiffness coefficients which take into account the orientation of each ply with respect to the wave propagation direction and are defined as

$$\begin{aligned} Q'_{11} &= m^4 Q_{11} + n^4 Q_{22} + 2m^2 n^2 Q_{12} + 4m^2 n^2 Q_{66} \\ Q'_{22} &= n^4 Q_{11} + m^4 Q_{22} + 2m^2 n^2 Q_{12} + 4m^2 n^2 Q_{66} \\ Q'_{12} &= m^2 n^2 Q_{11} + m^2 n^2 Q_{22} + (m^4 + n^4) Q_{12} - 4m^2 n^2 Q_{66} \end{aligned} \quad (45)$$

where $m = \cos(\theta)$ and $n = \sin(\theta)$. The angle θ is defined as positive for a counterclockwise rotation from the primed (laminated) axes to the unprimed (individual lamina) axes. From Eq. (5), the Q'_{ij} for the 0° and 90° laminas are given by

$$\begin{aligned} (Q'_{11})_{0 \text{ deg}} &= Q_{11} & (Q'_{11})_{90 \text{ deg}} &= Q_{22} \\ (Q'_{22})_{0 \text{ deg}} &= Q_{22} & (Q'_{22})_{90 \text{ deg}} &= Q_{11} \\ (Q'_{12})_{0 \text{ deg}} &= Q_{12} & (Q'_{12})_{90 \text{ deg}} &= Q_{12} \end{aligned} \quad (46)$$

The velocity of the extensional plate mode can be related to the in-plane stiffness of a composite for propagation in the 0° and 90° directions, these stiffnesses are A_{11} and A_{22} , respectively. The extensional plate mode velocity is related to the stiffness from Eq. (47) and Eq. (48), Prosser (1991).

$$\text{for propagation in the } 0^\circ \text{ direction } c_t = \sqrt{\frac{A_{11}}{\rho h}} \quad (47)$$

$$\text{for propagation in the } 90^\circ \text{ direction } c_l = \sqrt{\frac{A_{22}}{\rho h}} \quad (48)$$

The values for the inplane stiffnesses A_{11} and A_{22} can be calculated using Eqs. (42)-(46) if the engineering stiffnesses of the composite are known. Finally, Eq. (47) and Eq. (48) are substituted into Eq. (40) and it is solved numerically in MathematicaTH. For a given material, the Young's Module in the propagation direction as E_1 , E_2 , Poisson Ratio ν_{12} , and the density ρ are known, and the phase velocity (c_{phase}) is the dependent variable being solved for the independent variable being iteratively supplied is the frequency-thickness product, where ω is the driving frequency in radians. The very useful plot is the group velocity dispersion curve, which is derived from the phase velocity curve using Eq. (49)

$$c_{group} = c_{phase} + \frac{\partial c_{phase}}{\partial k} k = \frac{c_{phase}}{1 - \frac{f}{c_{phase}} \cdot \frac{\partial c_{phase}}{\partial f}} \quad (49)$$

where f is the frequency in Hz.

These dispersion curves are the key to describing and understanding the propagation of Lamb waves in a solid medium, and will be used in the coming sections to find damping capacity of a material.

6. Results and discussion

In this work a methodology has been proposed for finding damping capacity of a material using combined finite element and Lamb wave method. Fig. 9 shows the process flow diagram for the dynamic mechanical analysis of the method. The relationship between the material properties of a specimen and the velocity of the propagating Lamb wave is quite complex, however an understanding is necessary to design an appropriate method for finding damping capacity of a material. In the Lamb wave equation the first order wave velocity increases with the square root of the modulus, i.e., an increase in modulus slightly speeds the wave velocity. An increase in the density would have the opposite effect slowing wave velocity, as it appears in all the same terms as the modulus but on the reciprocal side of the divisor.

The AE velocities of the specimens are determined experimentally using ultrasonic pulse generator test setup and the Young's modulus is calculated by using Eq. (1) and thus obtained Young's modulus is substituted in Lamb wave model discussed in previous sections for finding dispersion characteristics and the same material properties are used for finite element model to determine natural frequencies. The group velocity (c_{gn}) at natural frequency (f_n) and thickness (h) is substituted in Eq. (50) to determine the phase shift and thus finding material damping capacity ($\text{Tan}\delta$). Dynamic mechanical analysis can be carried out using the same procedure by getting the E_o value from group velocity dispersion at iteratively supplied frequencies.

$$\delta = 2\pi f_n h / c_{gn} \quad (50)$$

$$E_o = c_{gn}^2 \cdot \rho \quad (51)$$

Damping is the term used in vibration and noise analysis to describe any mechanism whereby mechanical energy in the system is dissipated. The damping properties of so-called damping materials, such as elastomeric materials, are usually temperature and frequency dependent, so the experimental determination of damping material properties requires a long and repeating process.

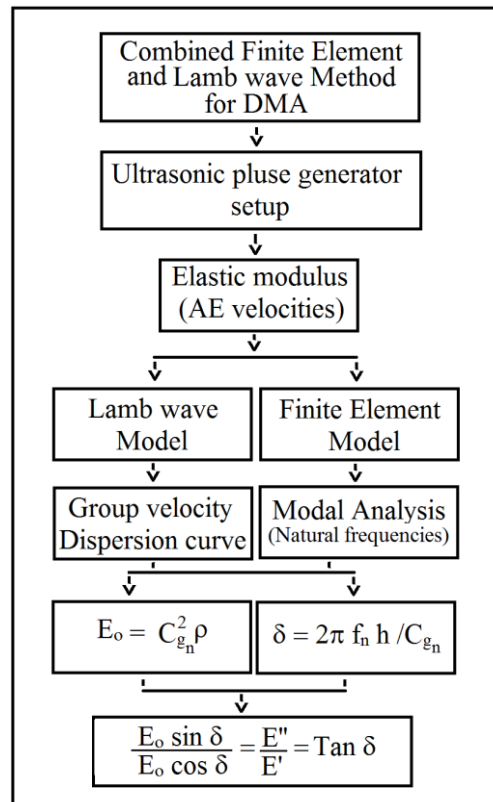


Fig. 9 Process flow diagram for dynamic mechanical analysis by Lamb wave method

Table 1 Material properties calculated using experimental setup

Material	V_T (m/s)	V_L (m/s)	ν_{12}	E_1 (Gpa)	E_2 (Gpa)	ν_{21}	Density (ρ) kg/m ³
GFRP	6439	3128	0.346	47.31	11.26	0.081	1853
CFRP	8745	4628	0.307	77.74	21.73	0.086	1400

Many researches carried damping measurements in temperature sweep mode but the present work involves frequency sweep since the damping is to eliminate the noise and vibrations resulting from natural frequencies in many industrial applications. In the present work damping measurements were carried out using combined finite element and Lamb wave method and the results were compared with bandwidth method. Both the methods were performed on same experimental setup and the materials properties of the test specimen obtained from experimental setup, reported in Table 1.

The modal analysis was carried out using developed finite element model and it was correlated with ANSYS. The waveform from the instrument is processed through virtual controlling software and the continuous waveform is subjected to fast Fourier transform (FFT) which yield a single peak from the calibrated optimal driving frequency, however for a few finite cycles, the FFT appears as a Gaussian curve. The response curve of the materials being tested for damping capacity using bandwidth method is shown in Fig. 10.

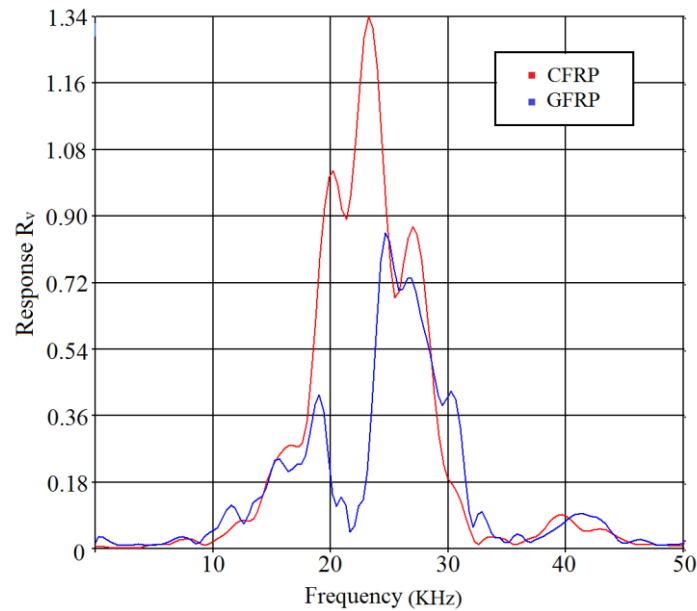


Fig. 10 Response curve of GFRP and CFRP showing bandwidth

Table 2 Damping capacity of the test specimens

Material	Natural frequency (Hz)	Lamb wave method (Damping capacity)	Mode frequency(Hz)	Bandwidth method (Damping capacity)
GFRP	172(1 st)	0.0000493	8692	0.001394
	9970(10 th)	0.0012204	11537	0.002427
	21606(20 th)	0.0043671	19248	0.004251
CFRP	223(1 st)	0.0000646	8706	0.004569
	11023(10 th)	0.0016254	20835	0.021765
	23158(20 th)	0.0516527	23164	0.049638

The Lamb wave dispersion curves have been obtained from the iterative supply of the frequency using MathematicaTH code. The group velocity dispersion curve of the material used in this research is shown in Fig. 11. The group velocities and the natural frequencies obtained from modal analysis are used to determine damping capacity at the mode of interest. Table 2 presents the damping capacities of the tested materials by Lamb wave method and Bandwidth method in comparison at critical modes. In case of Lamb wave method natural frequencies at different mode shape has been considered and in case of Bandwidth method changes in peaks is considered as mode frequency. It is observed that the Lamb wave method can be compared with the Bandwidth method at higher mode of frequencies. Fig. 12 shows the damping capacities and dynamic storage modulus of the tested specimens with respect to their natural frequencies. The material GFRP and CFRP exhibits similar damping property to a certain range of frequency, and in between 2 kHz to 8 kHz GFRP has better damping property among the two and at higher range of frequencies CFRP is found to be good in damping characteristics.

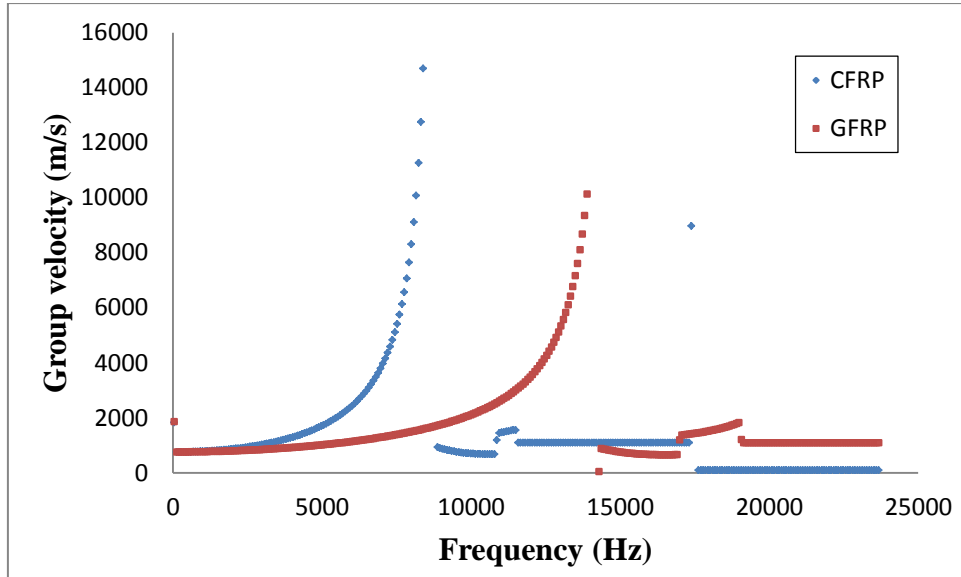


Fig. 11 Lamb wave dispersion curves of CFRP and GFRP

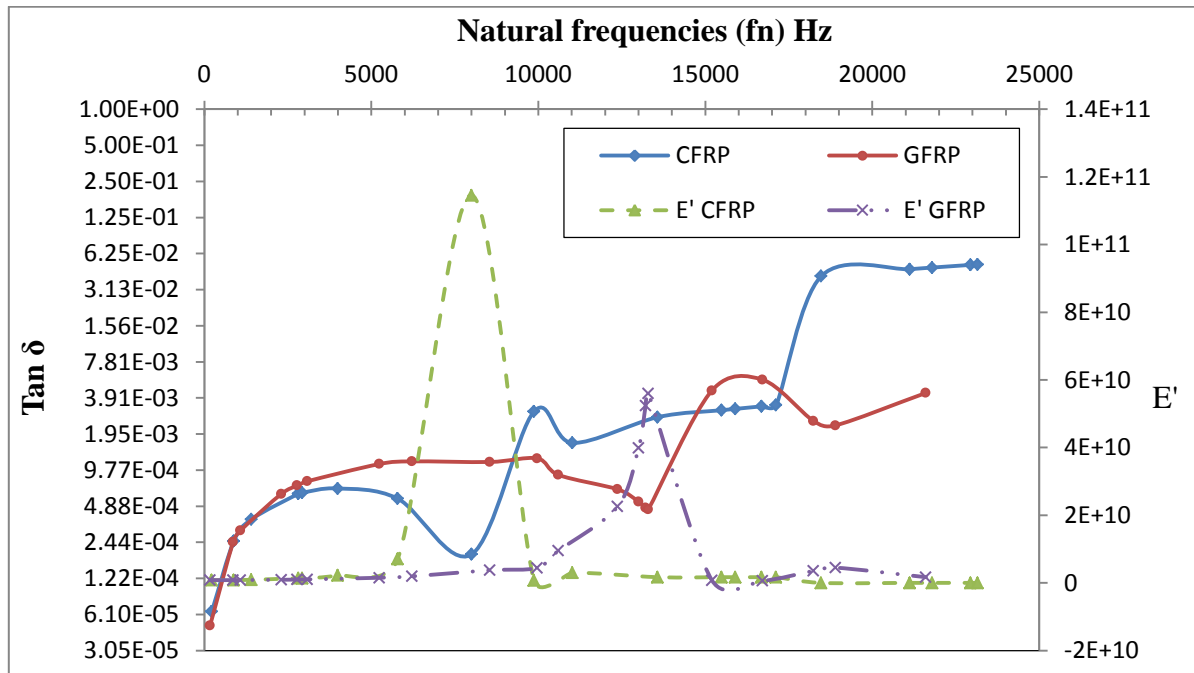


Fig. 12 Damping capacity and dynamic storage modulus for CFRP and GFRP

7. Conclusions

Dynamic mechanical analysis is a technique used to study and characterize materials. It is most useful for studying the viscoelastic behavior of polymers. Combined finite element and Lamb

wave method has been explored in this work and tests were carried out on CFRP and GFRP composite plates. The results of this method were compared with the results of the traditional bandwidth method and they were in close agreement. The main advantage of this method is that the materials can be tested in high frequency range, specifically at its natural frequencies and at relatively low amplitudes and in a non-distractive way.

Acknowledgements

This research was supported by Basic Science Research Program through the National Research Foundation of Korea(NRF) funded by the Ministry of Education(2010-0020089).

Reference

- Birt, E.A. (1998), "Damage detection in carbon-fibre composites using ultrasonic lamb waves", *Non-Destructive Test. Condition. Monit.*, **40**, 335-339.
- Blake, R.E. (2010), *Basic Vibration Theory*, Piersol A.G., Paez T.L. Harris' Shock and Vibration Handbook, 6th Edition, Mc-Graw Hill, New York.
- Botelho, E.C., Pardini, L.C. and Rezende, M.C. (2006), "Damping behavior of continuous fiber/metal composite materials by the free vibration method", *Compos. Part B*, **37**, 255-264.
- Chen, Y. and Gibson R.F. (2003), "Analytical and experimental studies of composite isogrid structures with integral passive damping", *Mech. Adv. Mater. Struct.*, **10**(2), 127-143.
- Dalton, R.P., Cawley, P. and Lowe, M.J.S. (2001), "The potential of guided waves for monitoring large areas of metallic aircraft fuselage structure", *J. Nondestr. Eval.*, **20**, 29-46.
- Daniel, I.M. and Ishai, O. (1994), *Engineering Mechanics of Composite Materials*, Oxford U.P, New York.
- Gibson, R.F. (1992), *Nontraditional Applications of Damping Measurements*, STP 1169 Mechanics and Mechanisms of Material Damping, Kinra, V.K., Wolfenden, A., Philadelphia.
- Gremaud, G., Kustov, S.L. and Bremnes, O. (2001), "Ultrasonics techniques: PUCOT and ACT", *Mater. Sci. Forum.*, **652**, 366-368.
- Guan, H. and Gibson, R.F. (2001), "Micromechanical models for damping in woven fabric-reinforced polymer matrix composites", *J. Compos. Mater.*, **35**(16), 1417-1434.
- Harmouche, M.R. and Wolfenden, A.J. (1985), *Test. Eval.*, **13**, 424-428.
- Krautkramer, J. and Krautkramer, H. (1983), *Ultrasonic Testing of Materials*, Berlin, Heidelberg, New York.
- Kwon, Y.W. (1989), "Finite element analysis of crack closure in plate bending", *Comput. Struct.*, **32**, 1439-1445.
- Marx, J. (1951), *Rev. Sci. Instrum.*, **22**, 503-509.
- McIntire, P. (1991), *Nondestructive Testing Handbook*, American Society for Nondestructive Testing, **7**, 398-402.
- Michael, W.H. (1998), *Stress Analysis of Fiber-Reinforced Composite Materials*, WCB McGraw-Hill.
- Mu, B., Wu, H.C., Yan, A., Warnemuende, K., Fu, G., Gibson, R.F. and Kim, D.W. (2006), "FEA of complex bridge system with FRP composite deck", *J. Compos. Construct.*, **10**(1), 79-86.
- Nowick, A.S. and Berry B.S. (1972), *Anelastic Relaxation in Crystalline Solids*, Academic Press, New York.
- Owen, D.R.J. and Li, Z.H. (1987), "A refined analysis of laminated plates by finite element displacement method - I fundamental and static analysis", *Comput. Struct.*, **26**, 907-914.
- Prosser, W.H. (1991), "The propagation characteristics of the plate modes of acoustic emission waves in thin aluminum plates and thin graphite/epoxy composite plates and tubes", NASA Technical Memorandum 104187.

- Ratnam, C., Ben, B.S. and Ben, B.A. (2009), "Structural damage detection using combined finite element and model lamb wave propagation parameters", *IMECHE Part C: J. Mech. Eng. Sci.*, **223**, 769-777.
- Summerscales, J. (1987), *Non-Destructive Testing of Fiber-Reinforced Plastics Composites*, Elsevier Applied Science, London and New York.